

Structure–Property Dependence of the First Hyperpolarisabilities of Organometallic Merocyanines Based on the μ -Vinylcarbonyliron Acceptor and Ferrocene Donor

Tony Farrell,^{*[a]} Anthony R. Manning,^{*[a]} Timothy C. Murphy,^[a] Timo Meyer-Friedrichsen,^[b] Jürgen Heck,^[b] Inge Asselberghs,^[c] and André Persoons^[c]

Keywords: Nonlinear optical materials / Ferrocene / Merocyanine / Hyper Rayleigh scattering / Solvatochromism / Bond-length alternation

In order to investigate the structure–property relationship of nonlinear optical materials, a series of organometallic chromophores were synthesised utilising the $[\text{Fe}_2(\eta\text{-C}_5\text{H}_5)_2(\text{CO})_2(\mu\text{-CO})(\mu\text{-C-})]^+$ electron-accepting moiety and the ferrocenyl group, Fc, as the electron donor. The π -linker between these two termini was systematically modified and the mutual electronic communication between them was determined using IR, NMR, and electronic absorption spectroscopy. An X-ray structure determination of $[\text{Fe}_2(\eta\text{-C}_5\text{H}_5)_2(\text{CO})_2(\mu\text{-CO})(\mu\text{-C-CH=CH-CH=C(Cl)-Fc})][\text{BF}_4]$ confirmed the strong electronic interaction between the donor and the acceptor with reduced π -bridge bond-length alternation. The nonlinear optical properties of these complexes were examined using the hyper Rayleigh scattering technique. The experimental first hyperpolarisabilities are some of the highest obtained for ferrocenyl chromophores and, significantly, no enhancement

was found due to two-photon absorption fluorescence. When polyene linkers $-(\text{CH=CH})_n-$ are used, the values for β_0 increase with a ca. $n^{1.5}$ dependence with no sign of saturation up to $n = 4$. However, the highest values for β and β_0 were obtained for linkers which contained an aromatic ring as opposed to pure polyenes and in this respect a benzene ring was more effective than a thiophene or furan. Consequently, the higher β and β_0 are not exhibited by those merocyanines with the highest values for λ_{max} . It is concluded for these compounds that a low excitation energy E_{eg} and a large transition moment M for the electronic excitation are less important than a large change in the dipole moment $\Delta\mu_{\text{eg}}$. Furthermore, a chloro substituent on the olefinic double bond proximate to the ferrocenyl group has a dramatic effect on the β and β_0 values.

Introduction

Molecular electronics is an emerging and intriguing area of research. Understanding the structure–property relationship of NLO-active chromophores is of fundamental importance if molecular architecture is to be tailored to achieve specific NLO responses. The strategy requires sequential variation of molecular parameters, full evaluation of the effects which these variations have on the ground and excited states, and then analysing the outcome on the NLO response. Organic systems have been subject to extensive studies whereby the effects of modulating such variables as spacer aromaticity, bond-length alternation, and end-group donor and acceptor strengths have been quantified.^[1–7] Less work has been carried out on organometallic chromophores despite the fact that organometallic complexes are often particularly appealing because their redox states may be changed easily. However, there are now increasing numbers of ferrocenyl complexes which display

interesting molecular electronic functions such as nonlinear optical (NLO) properties (including frequency doubling and tripling of incident light),^[8–13] and metallocenes have been used in amperometric sensory devices^[14] and liquid crystals.^[15,16]

One of our approaches has been to synthesise complexes which utilise the cationic diiron moiety $[\text{Fe}_2(\eta\text{-C}_5\text{H}_5)_2(\text{CO})_2(\mu\text{-CO})(\mu\text{-C-})]^+$ moiety, as an electron acceptor in molecular systems which are candidates for second harmonic generation (SHG). This end-group is particularly attractive because theoretical^[17] and experimental^[18–22] research has indicated that conjugation between the $\text{Fe}_2(\mu\text{-C})$ unit and the substituted vinyl system is maintained throughout rotation about the $\mu\text{-C-vinyl}$ bond.

Hyper Rayleigh scattering (HRS) studies using 1064 nm incident light on the stilbenyldiiron series $[\text{Fe}_2(\eta\text{-C}_5\text{H}_5)_2(\text{CO})_2(\mu\text{-CO})(\mu\text{-C-CH=CH-C}_6\text{H}_4\text{-CH=CH-C}_6\text{H}_4\text{-R})][\text{BF}_4]$ (where $\text{R} = \text{NO}_2, \text{H}, \text{OMe}, \text{NMe}_2$), were promising.^[22] Based on these findings the objective of this work was to prepare a comparable series of merocyanines utilising the diiron cationic electron acceptor and ferrocene as the donor. It was proposed that modifications of the π -bridge between these termini by incorporating olefins and aryl or heteroaryl units as well as more subtle changes, i.e. replacing an H atom on an olefinic unit by a Cl atom along

[a] Department of Chemistry, University College Dublin, Belfield, Dublin 4, Ireland

[b] Institut für Anorganische und Angewandte Chemie, Universität Hamburg, Martin-Luther-King-Platz 6, 20146 Hamburg, Germany

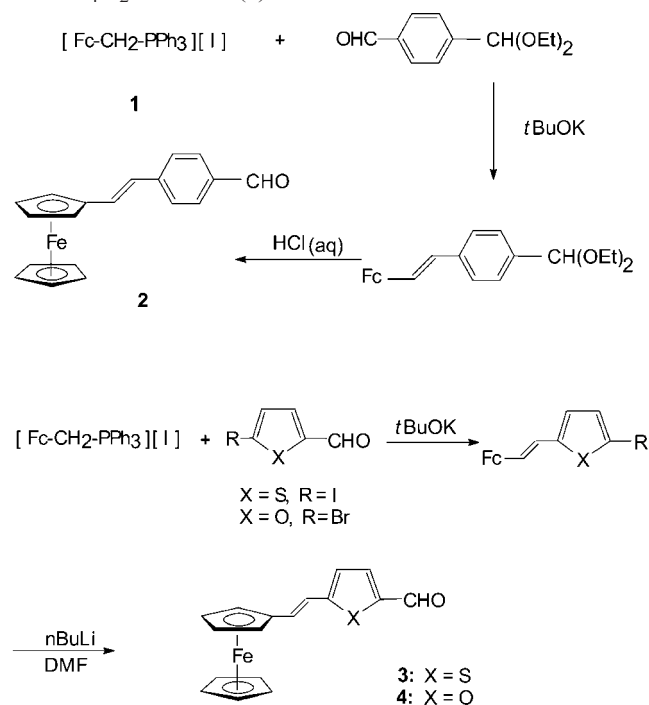
[c] Laboratorium voor chemische en biologische dynamica, Katholieke Universiteit Leuven, Celestijnenlaan 200D, 3001 Leuven, Belgium

the π -linker, could give systems which exhibit large second-order NLO effects and would help to clarify the criteria necessary to achieve this.^[23–26]

Results and Discussion

Synthesis

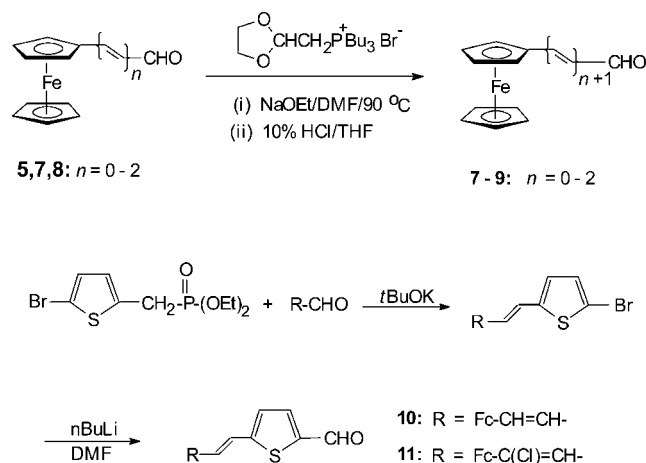
Wittig condensation of terephthalaldehyde mono(diethyl acetal) with an equimolar amount of the phosphonium salt $[\text{Fc}-\text{CH}_2-\text{PPh}_3][\text{I}]$ (**1**)^[27,28] and *t*BuOK, provided the acetal $\text{Fc}-\text{CH}=\text{CH}-\text{C}_6\text{H}_4-\text{CH}(\text{OEt})_2$ which was not isolated but immediately converted into the aldehyde $\text{Fc}-\text{CH}=\text{CH}-\text{C}_6\text{H}_4-\text{CHO}$ (**2**) by treating with aqueous HCl (Scheme 1). Wittig condensation of **1** with 5-iodothiophene-2-carboxaldehyde^[29–31] and 5-bromofuryl-2-carboxaldehyde^[29,32,33] followed by lithium/halogen exchange and DMF quenching gave the heteroarylferrocenyl aldehydes $\text{Fc}-\text{CH}=\text{CH}-\text{C}_4\text{H}_2\text{S}-\text{CHO}$ (**3**) and $\text{Fc}-\text{CH}=\text{CH}-\text{C}_4\text{H}_2\text{O}-\text{CHO}$ (**4**).



Scheme 1. Synthesis of ferrocenyl aldehydes **2–4**

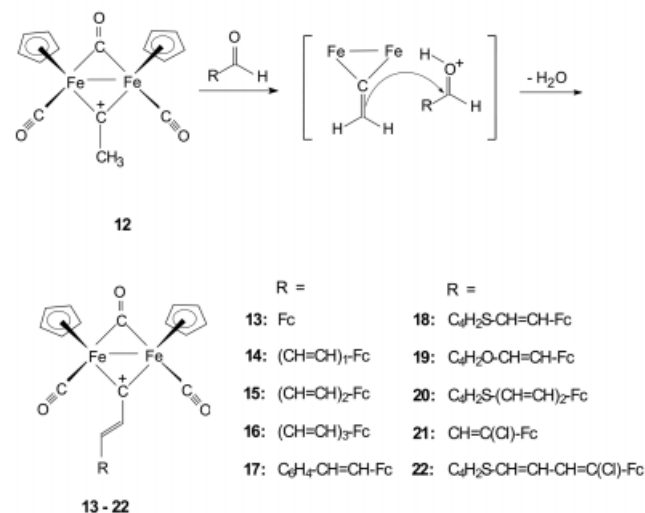
Ferrocene aldehyde^[34] **5** and (chlorovinyl)ferrocene aldehyde^[35] **6** were prepared by known procedures while the extended [formyl(vinyl)]_nferrocenes **7–9** were obtained by the method of Spangler and McCoy (Scheme 2).^[36] The extended vinylthienyl aldehydes $\text{Fc}-\text{CH}=\text{CH}-\text{CH}=\text{CH}-\text{C}_4\text{H}_2\text{S}-\text{CHO}$ (**10**) and $\text{Fc}-\text{C}(\text{Cl})=\text{CH}-\text{CH}=\text{CH}-\text{C}_4\text{H}_2\text{S}-\text{CHO}$ (**11**) were prepared by a Wittig–Horner–Wadsworth–Emmons procedure using diethyl [(2-bromothiophenyl)methyl]phosphonate^[22] (Scheme 2). As before, lithium/halogen exchange followed by DMF quenching afforded **10** and **11** in high yields. All ferrocenyl

aldehydes were characterised by ¹H NMR spectroscopy and exhibited signals, which were consistent with all-(*E*) geometries.



Scheme 2. Synthesis of ferrocenyl aldehydes **7–11**

When the aldehydes **2–11** were condensed with $[\text{Fe}_2(\eta-\text{C}_5\text{H}_5)_2(\text{CO})_2(\mu-\text{CO})(\mu-\text{C}-\text{CH}_3)][\text{BF}_4]$ (**12**) in CH_2Cl_2 at 35 °C for 12 h, they gave intensely coloured reaction mixtures. The air-stable merocyanine salts $[\text{Fe}_2(\eta-\text{C}_5\text{H}_5)_2(\text{CO})_2(\mu-\text{CO})(\mu-\text{C}-\{\pi\text{-linker}\}-\text{Fc})][\text{BF}_4]$, **13–22**, were isolated by filtering the reaction mixture and layering the filtrate with diethyl ether (Scheme 3). The complexes **13–22** were fully characterized by spectroscopic and elemental analysis. However, some of the products contained solvent of crystallization that could not be removed by vacuum drying. This was confirmed by NMR spectroscopy that revealed varying amounts of CH_2Cl_2 , diethyl ether and/or water. No attempt was made to quantify this solvent of crystallisation and the microanalytical data are given as found. However, the spectroscopic data are in agreement with the proposed formulae and we are confident of them.



Scheme 3. Reactions of **12** with ferrocenyl aldehydes **2–11**

Crystal Structure of $[\text{Fe}_2(\eta\text{-C}_5\text{H}_5)_2(\text{CO})_2(\mu\text{-CO})(\mu\text{-C-CH=CH-CH=C(Cl)-Fc)][\text{BF}_4]$ (**21**)

Suitable crystals of **21** were grown from a $\text{CH}_2\text{Cl}_2/\text{OEt}_2$ solution and subjected to an X-ray diffraction study. Crystal data and structure refinement are given in Table 5. A perspective view of the molecule and its atom numbering is depicted in Figure 1. Selected bond lengths and angles are listed in Table 1. The $\text{Fe}_2(\eta\text{-C}_5\text{H}_5)_2(\text{CO})_2(\mu\text{-CO})(\mu\text{-C})$ moiety has a *cis* structure with dimensions similar to those found in other μ -vinylcarbyne cations.^[22,38,39] The -CH=CH-CH=C(Cl)- π -bridge linker displays all-(*E*) geometry with C15–C16 and C17–C18 bond lengths of 1.359(5) and 1.356(5) Å respectively, which are rather long for $\text{C}_{\text{sp}^2}\text{-C}_{\text{sp}^2}$ double bonds. Furthermore, there is a shortening of the $\text{C}_{\text{sp}^2}\text{-C}_{\text{sp}^2}$ single bonds towards the diiron terminus [C14–C15 = 1.414(5), C16–C17 = 1.424(9), and C18–C19 = 1.447(9) Å], which is evidence for the delocalisation of the positive charge into the vinylcarbyne system and particularly through the first double bond in the solid state.^[19–21] This is particularly important because bond-length alternation (BLA, the difference between the average lengths of carbon–carbon single and double bonds in a merocyanine) has been established as a useful parameter in relation to NLO response.^[23,40,41] A good correlation between theory and experiment led to the conclusion that optimal NLO activity is achieved when BLA = 0.03–0.05 Å. The BLA across the π -bridge of **21** is 0.07 Å, which indicates a potentially high first hyperpolarisability.

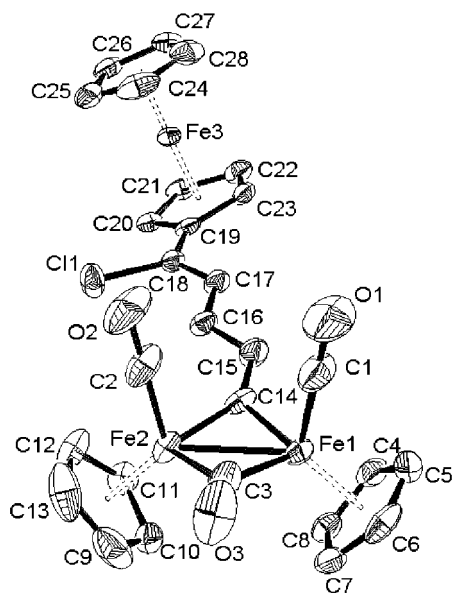


Figure 1. Molecular structure and atom labelling of $[\text{Fe}_2(\eta\text{-C}_5\text{H}_5)_2(\text{CO})_2(\mu\text{-CO})(\mu\text{-C-CH=CH-CH=C(Cl)-Fc)][\text{BF}_4]$ (**21**); 30% ellipsoids; hydrogen atoms and $[\text{BF}_4]^-$ anion omitted for clarity

Further evidence for the π -interaction between the diiron moiety and the first double bond is the planarity of the $\text{Fe}_2(\mu\text{-C})$ and C14–C16 units with the dihedral angle between their best planes being only 1.5(6)°. The entire π -

linker (C14–C19) is also quite planar with C17 and C14 displaying greatest deviations [+10.4(3) and –10.1(2)°, respectively] and a dihedral angle of 9.2(7)° between the best planes through C14–C16 and C17–C19. Nonetheless, the dihedral angle of 24.3(2)° between the C19–C23 (ferrocenyl $\eta\text{-C}_5\text{H}_4$) and the $\text{Fe}_2(\mu\text{-C})$ planes suggests that the ground state (GS) electronic delocalisation within the cation is effected mainly via the π -bridge with only a limited contribution from the ferrocenyl end group.

Spectroscopy

The solution IR spectra of complexes **13–22** contain three absorption bands in the $\nu(\text{CO})$ region (Table 2). Their relative intensities are consistent with the presence of a *cis*- $\text{Fe}_2(\eta\text{-C}_5\text{H}_5)_2(\text{CO})_2(\mu\text{-CO})(\mu\text{-C})$ moiety similar to those found in other $[\text{Fe}_2(\eta\text{-C}_5\text{H}_5)_2(\text{CO})_2(\mu\text{-CO})(\mu\text{-C-R})]^+$ complexes.^[19–22,38,39] The frequencies of these bands are a good indication of the electronic coupling between the $\text{Fe}_2(\mu\text{-C})$ electron accepting moiety and the vinylferrocenyl complex donor system. Increased electron density at the diiron terminus results in increased $\text{M}\rightarrow\text{CO}$ back donation with a concomitant shift of the $\nu(\text{CO})$ bands to lower frequencies. The $\nu(\text{CO})$ vibrations of the vinylcarbyne complexes **13–22** are found at lower frequencies than those of $[\text{Fe}_2(\eta\text{-C}_5\text{H}_5)_2(\text{CO})_2(\mu\text{-CO})\{\mu\text{-C-CH=CHC}(\text{CH}_3)_3\}][\text{BF}_4]$ ^[19] (**23**) (2036, 2003, 1853 cm^{-1}) and at very much lower frequencies than those of $[\text{Fe}_2(\eta\text{-C}_5\text{H}_5)_2(\text{CO})_2(\mu\text{-CO})(\mu\text{-C-CH}_3)][\text{BF}_4]$ ^[19] (**12**) (2047, 2016, 1853 cm^{-1}). They demonstrate that in the ground state (GS), (i) extension of the π -linker with polarisable olefinic units increases the positive charge at the $\text{Fe}_2(\mu\text{-C})$ core, (ii) when aromatic groups are included in the spacer, the delocalisation of this positive charge decreases with increasing aromaticity of that group, and (iii) the CH=C(Cl)-Fc unit is a weaker donor than CH=CH-Fc .

The spectra also display the expected absorption bands due to the BF_4^- ion and some unexpectedly strong bands lying between 1450 and 1600 cm^{-1} . The intensities of the latter are comparable to those of the $\nu(\text{CO})$ modes e.g. for **21** they are found at 1553 (4.6) and 1521 (13.1) cm^{-1} [relative intensities with $\nu(\text{CO})$ set to 10]. As they are not present in the IR spectrum of **12**, they are attributed to the $\nu(\text{C}=\text{C})$ and other internal vibrations of the vinylferrocenyl ligand. Their enhanced intensities is a consequence of the high degree of polarisation within the π -system of the molecule.

The ^1H NMR spectra of **13–22** are consistent with the proposed structures. In particular, the ^1H – ^1H coupling constants across all the olefinic CH=CH units ($J > 13.5$ Hz), confirm an (*E*) configuration in all cases. Although the two C_5H_5 ligands of the diiron unit are formally in different environments, a single resonance is observed in the ^1H NMR spectra of all the complexes. This suggests that in all cases there is facile rotation about the $\mu\text{-C-CH}$ bond which has a low bond order and is close to a single bond. This is consistent with the X-ray data discussed above. The protons of the ferrocenyl C_5H_4 ring appear as two broad resonances downfield from the singlet due to its C_5H_5 group. The

Table 1. Selected bond lengths [pm] and angles [°] for $[\text{Fe}_2(\eta\text{-C}_5\text{H}_5)_2(\text{CO})_2(\mu\text{-CO})\{\mu\text{-C}-\text{CH}=\text{CH}-\text{CH}=\text{C}(\text{Cl})-\text{Fc}\}][\text{BF}_4]$ (**21**)

Bond lengths		Bond angles	
Fe(1)–C(1)	177.5(5)	Fe(1)–[C4–C8] ^[a]	174.8(3)
Fe(1)–C(3)	192.2(3)	Fe(2)–[C9–C13] ^[b]	174.8(3)
Fe(1)–C(14)	184.3(5)	Fe(1)–C(3)–Fe(2)	80.8(2)
Fe(2)–C(2)	176.8(4)	Fe(1)–C(14)–Fe(2)	85.6(2)
Fe(2)–C(3)	194.9(4)	C(14)–C(15)–C(16)	122.4(4)
Fe(2)–C(14)	185.2(5)	C(15)–C(16)–C(17)	122.5(3)
Fe(1)–Fe(2)	250.9(11)	C(16)–C(17)–C(18)	120.1(5)
C(1)–O(1)	114.4(6)	C(16)–C(17)–C(22)	125.2(3)
C(2)–O(2)	114.2(5)	C(17)–C(18)–C(19)	124.7(3)
C(3)–O(3)	116.4(5)	C(17)–C(18)–Cl(1)	119.6(3)
C(14)–C(15)	141.4(5)	[Fe(1)–C(14)–Fe(2)][C(14)–C(16)]	1.5(6)
C(15)–C(16)	135.9(5)	[C(14)–C(16)][C(17)–C(19)] ^[c]	9.2(7)
C(16)–C(17)	142.4(5)	[C(19)–C(23)][C(14)–C(19)] ^[c]	23.1(3)
C(17)–C(18)	135.6(5)	[Fe(1)–C(14)–Fe(2)][C(19)–C(23)]	24.3(2)
C(18)–C(19)	144.7(5)		
C(18)–Cl(1)	174.0(3)		
C(20)–C(21)	138.5(8)		

^[a] Center of the Cp ring C(4)–C(8). – ^[b] Center of Cp ring C(9)–C(13). – ^[c] Angle between the two planes.

Table 2. Solution IR and ^{13}C NMR spectroscopic data for the $[\text{Fe}_2(\eta\text{-C}_5\text{H}_5)_2(\text{CO})_2(\mu\text{-CO})\{\mu\text{-C}-(\pi\text{-linker})-\text{Fc}\}][\text{BF}_4]$ salts **13–22**

	$\pi\text{-linker}$	IR (cm^{-1}) ^[a]		^{13}C NMR (ppm)
		$\nu(\text{CO})$	$\nu(\mu\text{-CO})$	$\mu\text{-C}$
13		2024, 1993	1837	408 ^[b]
14		2027, 2001	1837	411 ^[b]
15		2028, 2000	1837	414 ^[b]
16		2029, 2001	1839	416 ^[b]
17		2035, 2004	1844	432 ^[c]
18		2030, 1999	1839	410 ^[c]
19		2029, 2000	1838	407 ^[c]
20		2030, 2000	1839	414 ^[b]
21		2031, 2001	1841	423 ^[d]
22		2031, 2001	1840	421 ^[b]

^[a] CH_2Cl_2 . – ^[b] $(\text{CD}_3)_2\text{CO}$. – ^[c] CDCl_3 . – ^[d] CD_3CN .

chemical shift of these signals depends on the interaction between the ferrocenyl electron donor and the cationic diiron terminus and is related to both the length and the ease of polarisation of the bridge. For example, as the $\pi\text{-linker}$ in the $[\text{Fe}_2(\eta\text{-C}_5\text{H}_5)_2(\text{CO})_2(\mu\text{-CO})\{\mu\text{-C}-(\text{CH}=\text{CH})_n-\text{Fc}\}]^+$ cations is extended from $n = 1$ to $n = 4$, the C_5H_4 ^1H NMR signals are shifted 0.71 ppm upfield.

The ^{13}C NMR spectra of **13–22** exhibit all the anticipated resonances, but the most informative are those due to the $\mu\text{-C}$ atom ($\delta = 408\text{--}432$, Table 2). They are highly shielded relative to the $\mu\text{-C}$ signal of **12** ($\delta = 499$), but deshielded compared with the $\mu\text{-C}$ signal of alkenyldenediiron complexes $[\text{Fe}_2(\eta\text{-C}_5\text{H}_5)_2(\text{CO})_2(\mu\text{-CO})(\mu\text{-C}=\text{CH}-\text{R})]$ ($\delta = 270\text{--}340$).^[18,21,22,42–45] The greater the degree of charge delocalisation within the $\mu\text{-carbyne}$ moiety of the cation, the more pronounced is the upfield shift of this signal which will therefore depend on the length and ease of polarisation of the $\pi\text{-linker}$. The effect of $\pi\text{-bridge}$ modification on the chemical shift of the $\mu\text{-C}$ resonance can be summarised as follows: (i) increasing conjugation by adding olefinic units results in a slight downfield shift, (ii) replacing a heteroaryl $\pi\text{-spacer}$ by the more aromatic benzenoid unit also results in a downfield shift and (iii) replacing the $\text{CH}=\text{CH}$ proximate to the ferrocene by a $\text{CH}=\text{C}(\text{Cl})$ unit produces an upfield shift. Thus the electron donating effect of the ferrocenyl group in the GS decreases with donor–acceptor separation, the presence of aromatic $\pi\text{-spacers}$ and the increasing electronegativity of the bridge carbon atom α to it.

The UV/Vis spectra of **13–22**, like those of most ferrocenyl derivatives, exhibit two intense absorption bands in the visible region (Table 3).^[8–12,46–49] Figure 2 demonstrates the effect of $\pi\text{-bridge}$ extension on the absorption spectra of $[\text{Fe}_2(\eta\text{-C}_5\text{H}_5)_2(\text{CO})_2(\mu\text{-CO})\{\mu\text{-C}-(\text{CH}=\text{CH})_n-\text{Fc}\}]^+$. Both bands are red-shifted with increasing polyenic chain length but this is more pronounced for the

Table 3. Optical data for the $[\text{Fe}_2(\eta\text{-C}_5\text{H}_5)_2(\text{CO})_2(\mu\text{-CO})\{\mu\text{-C}-(\pi\text{-linker})\text{-Fc}\}][\text{BF}_4]$ salts **13–22**

	λ_{max} [nm] (ϵ [$\text{M}^{-1}\text{cm}^{-1}$])		λ_{max} [nm] (ϵ [$\text{M}^{-1}\text{cm}^{-1}$])		$\Delta\tilde{\nu}^{[a]}$ [cm^{-1}]		$\beta^{[b]}$ [10^{-30} esu]	$\beta_0^{[c]}$ [10^{-30} esu]
	CH_2Cl_2 DA–CT	CH_2Cl_2 LL–CT	CH_3CN DA–CT	CH_3CN LL–CT	DA–CT	LL–CT		
13	655 (10 953)	428 (17 736)	634 (9 390)	421 (15 245)	–506	–388	113	36
14	734 (13 881)	484 (17 094)	698 (10 029)	471 (14 397)	–703	–570	156	74
15	775 (18 277)	541 (22 488)	717 (16 275)	508 (21 034)	–1 044	–1 201	227	120
16	813 (23 106)	582 (24 670)	720 (14 954)	521 (21 678)	–1 589	–2 012	562	313
17	705 (12 162)	512 (28 692)	616 (12 803)	480 (26 773)	–2 049	–1 302	1 106	469
18	757 (19 966)	569 (32 538)	688 (17 147)	542 (26 378)	–1 324	–875	679	343
19	747 (22 325)	577 (33 211)	683 (21 202)	551 (28 946)	–1 254	–818	352	173
20	764 (22 363)	606 (29 169)	677 (19 199)	590 (30 565)	–1 682	–448	1 195	615
21	746 (17 173)	495 (27 589)	713 (13 986)	477 (24 439)	–620	–762	459	225
22	731 (24 000)	606 (34 798)	644 (30 695)	572 (36 213)	–1 848	–981	1 424	674

^[a] $\Delta\tilde{\nu} = (\tilde{\nu}_{\text{max}} \text{ in } \text{CH}_2\text{Cl}_2 - \tilde{\nu}_{\text{max}} \text{ in } \text{CH}_3\text{CN})$. – ^[b] Measured in CH_2Cl_2 with ref. *p*-NA ($\beta = 21.6 \cdot 10^{-30}$ esu). – ^[c] Calculated from the TLM using the lower energy CT band.

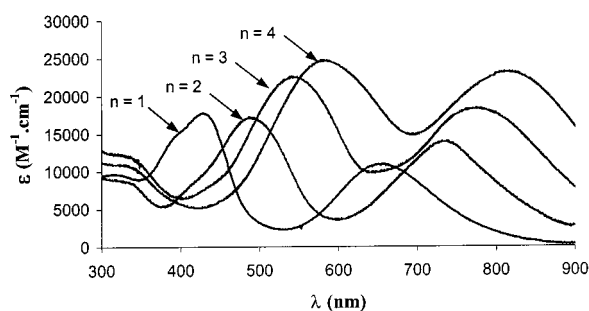


Figure 2. Effect of π -bridge extension on the absorption spectra of the $[\text{Fe}_2(\eta\text{-C}_5\text{H}_5)_2(\text{CO})_2(\mu\text{-CO})(\mu\text{-C}-(\text{CH}=\text{CH})_n\text{-Fc})][\text{BF}_4]$ salts **13–16**

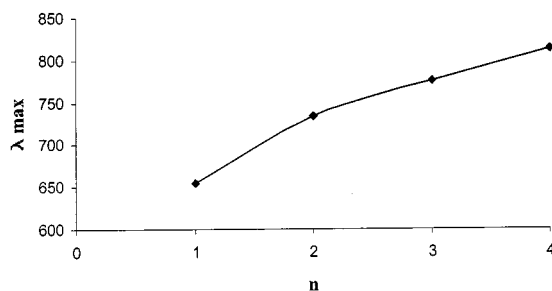


Figure 3. The variation of λ_{max} of the DA–CT absorption band of the $[\text{Fe}_2(\eta\text{-C}_5\text{H}_5)_2(\text{CO})_2(\mu\text{-CO})(\mu\text{-C}-(\text{CH}=\text{CH})_n\text{-Fc})][\text{BF}_4]$ salts **13–16**, with increasing n

higher energy band. In the case of organic donor–acceptor dyes, extending the π -linker results in the CT band moving to a limiting value known as the merocyanine limit (Figure 3).^[50] Therefore we suggest that the low-energy band is probably due to a donor–acceptor transition (DA–CT) and the higher energy band to an intraligand $\pi\text{-}\pi^*$ transition (LL–CT). Many contrasting theoretical models have attempted to describe the electronic origin of these bands and their contribution to the second-order response.^[51–53] Our assignments are in agreement with the most recent of these.^[53]

The wavelengths of both absorption bands in the electronic spectra of **13–22** are solvent-dependent (Table 3).

This is important because theoretical and experimental results suggest that the performance of NLO chromophores is optimised when there is a large difference between the dipole moments of the ground state (GS) and the excited state (ES) of the system.^[54,55] and solvatochromism of the CT bands of chromophores is considered a manifestation of this change in dipole moment upon excitation.^[50] In the case of **13–22** both bands are significantly blue-shifted with increasing solvent polarity (Figure 4 and Table 3). This indicates a large change in dipole moment upon excitation from a more charge-localised GS with a high dipole moment to an excited state where the positive charge is more delocalised throughout the entire molecule and the dipole moment is lower. In **13–16** the distance between donor and acceptor is increased by inserting more $\text{CH}=\text{CH}$ units into the linker. Consequently it is not surprising that the solvatochromic shifts $\Delta\tilde{\nu}$ also increase along the same series as dipole moments are a function of charge and distance. Furthermore, when the benzene spacer in **17** is replaced by a thiophene in **18** or a furan in **19**, the charge delocalisation in the GS is increased, the dipole moment change on excitation is reduced, and so is the solvatochromic shift (Table 3). At the same time, one would expect a decrease in solvatochromism upon incorporation of heterocycles into the π -linker because of their ability to act as auxiliary donors within the bridge.^[3–6,22]

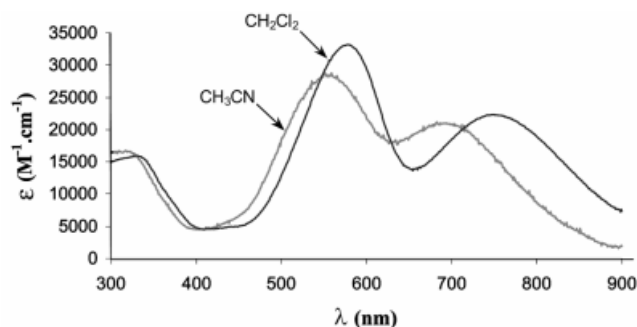


Figure 4. Solvatochromic behaviour of $[\text{Fe}_2(\eta\text{-C}_5\text{H}_5)_2(\text{CO})_2(\mu\text{-CO})(\mu\text{-C}-\text{CH}=\text{CH}-\text{C}_4\text{H}_2\text{O}-\text{CH}=\text{CH}-\text{Fc})][\text{BF}_4]$ (**19**)

Another notable feature is the effect of replacing the $-\text{CH}=\text{CH}-$ double bond proximate to the metallocene by a $-\text{CH}=\text{C}(\text{Cl})-$ unit. This increases the electronegativity of the ferrocenyl α -carbon atom and reduces the electron-donating capability of the ferrocenyl unit. If we consider that mesomers **A** and **B**, and to a lesser extent **C**, are the principal contributors to the GS of the diene π -bridged complexes **14** and **21** (Figure 5), then replacing $\text{X} = \text{H}$ by $\text{X} = \text{Cl}$ significantly reduces the stability of **C** and its contribution to the overall GS structure. Reduced charge delocalisation has the effect of raising the HOMO and we can presume that it also raises the energy of the LUMO, as mesomer **C** contributes substantially to the ES. Inspection of the spectra shows that on going from **14** to **21** there is (i) a downfield shift of the $\mu\text{-C}$ signal in the ^{13}C NMR spectrum, (ii) an increase of the frequencies of the $\nu(\text{CO})$ modes, (iii) a red-shift of the λ_{max} of the DA-CT band, and (iv) a decrease of its solvatochromism. These observations show that the second olefinic unit contributes significantly to charge delocalisation in the GS and that perturbing it has a significant effect on the HOMO.

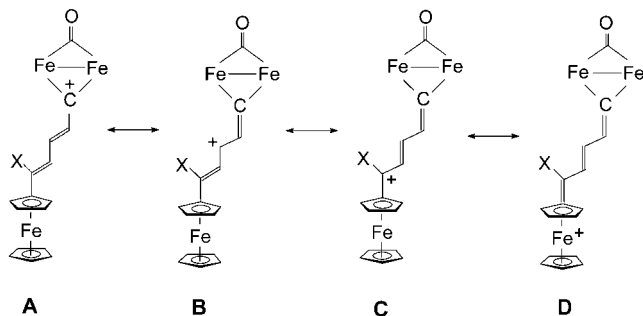


Figure 5. Four mesomeric forms of **14** and **21** (C_5H_5 and CO ligands omitted for clarity)

The same structural modification but in the extended π -bridged complexes incorporating a thienyl group, i.e. **20** and **22**, has a different effect. The IR and NMR spectroscopic data suggest that electronic communication between the termini is reduced upon incorporation of the aromatic heterocycle but that there are only minor changes in the degree to which positive charge is delocalised away from the $\text{Fe}_2(\eta\text{-C}_5\text{H}_5)_2(\text{CO})_2(\mu\text{-CO})(\mu\text{-C}^+)$ group. However, the electronic absorption spectra suggest that introduction of the chloro substituent affects the LUMO on going from **20** to **22** and brings about a blue-shift of the DA-CT band.

Hyperpolarisability Measurements

The NLO properties of **13–22** were evaluated by the hyper Rayleigh scattering (HRS) technique to determine their first hyperpolarisability β .^[56] This technique involves detecting the incoherently scattered frequency-doubled light $I(2\omega)$ generated from a solution of the sample. Several different concentrations of solute are taken so as to eliminate possible solvent contributions, which are generally linear. The dependence of the ratio $I(2\omega)/I(\omega)^2$ from the concentration of the NLO chromophore referred against a standard leads to the $\beta(\text{HRS})$ value.

There are certainly pitfalls associated with the technique which, if unchecked, lead to overestimation of the β values. Nonetheless, it remains the easiest means of assessing the first hyperpolarisability of ionic and octupolar molecules.^[57] The most common source of unreliable results is from two-photon fluorescence absorption (TPAF).^[58–61] However, there are now several methods which may be used to discriminate between a true SHG signal and a TPAF-enhanced one, e.g. the use of bandpass filters^[12,22] or a scanning monochromator.^[62] Also, numerous techniques have been developed to avoid or abstract the TPAF contribution to β : long wavelength measurement,^[63–65] time-resolved HRS,^[66] high-frequency demodulation^[67] and the measurement of the TPAF spectrum to abstract the fluorescence contribution to the HRS signal.^[68,69]

The HRS experiments were carried out in CH_2Cl_2 solution at 1064 nm fundamental wavelength using *p*-nitroaniline (*p*NA) as an external reference. The calculated β values of the complexes **13–22** are presented in Table 3. These values are resonance-enhanced and therefore the static first hyperpolarisabilities (β_0) have been calculated using the two-level model [TLM, Equation (1)].^[54,55] We have reservations about using the TLM to calculate β_0 as (i) strictly speaking, it is not applicable in situations where there is significant absorption near the SHG signal (532 nm) and (ii) the relative contributions of the two transitions in metallocene chromophores are still uncertain with the latest study reporting that both transitions contribute significantly to the optical nonlinearity.^[53] Nonetheless, to allow comparisons to be drawn between these complexes and the rest of the body of work on ferrocenyl systems we calculate the β_0 values using the lower energy CT transition (Table 4).

$$\beta_{\text{CT}}(-2\omega, \omega, \omega) = \frac{3\Delta\mu_{\text{eg}}M^2}{(\hbar\omega)^2} \cdot \frac{\omega_{\text{eg}}^2}{(1 - 4\omega^2/\omega_{\text{eg}}^2)(\omega_{\text{eg}}^2 - \omega^2)} \quad (1)$$

$$\beta_0 = \frac{3\Delta\mu_{\text{eg}}M^2}{(E_{\text{eg}})^2}$$

To ensure that the calculated values are real, a check for multiphoton-induced fluorescence enhancement was undertaken using bandpass filters at $\lambda = 400, 450, 500, 532, 560, 650,$ and 700 nm with a bandwidth of 10 nm as reported earlier.^[22] A fluorescence signal should have a considerably broader line than the sharp HRS signal (Figure 6) and the maximum of the emission band occurs infrequently at $\lambda/2$.^[62,68,69] Overall the β values obtained for this series of cationic ferrocenyl chromophores are exceptionally high, but they have been rigorously checked for TPAF and show no enhancement.

There are two points of general interest in the values of β and β_0 (Table 3). Firstly, those of the $[\text{Fe}_2(\eta\text{-C}_5\text{H}_5)_2(\text{CO})_2(\mu\text{-CO})\{\mu\text{-C}-(\text{CH}=\text{CH})_n\text{-Fc}\}][\text{BF}_4]$ (**13–16**) complexes increase on lengthening the π -system with olefinic units, and a plot of $\log n$ against $\log \beta_0$ (Figure 7)

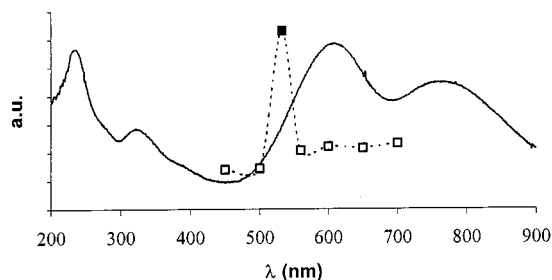


Figure 6. Absorption (full) and emission (dotted) spectra of the $[\text{Fe}_2(\eta\text{-C}_5\text{H}_5)(\text{CO})_2(\mu\text{-CO})\{\mu\text{-C-CH=CH-C}_4\text{H}_2\text{S-(CH=CH)}_2\text{-Fc}\}][\text{BF}_4]$ (**20**) in CH_2Cl_2 ; filled square is $\lambda = 532$ nm signal

shows that $\beta_0 \propto n^{1.5}$. This confirms that the static first hyperpolarisability of donor–acceptor polyene systems rise sharply with the length of the conjugated path. Furthermore, there is no evidence for the “saturation” of the β_0 enhancement with n increasing to 4, unlike λ_{max} , which is levelling off (Figure 3). In view of our results coupled with the linear optical data it would appear that the enhancement of β_0 for these cationic merocyanines could be largely attributed to $\Delta\mu_{\text{eg}}$, and M and less on the energy of the transition E_{eg} .

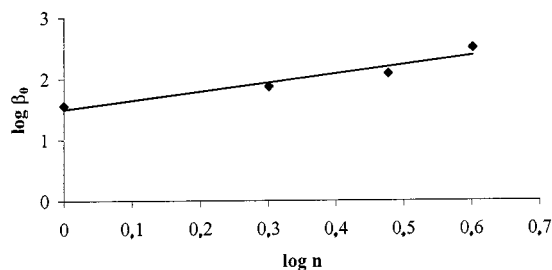


Figure 7. Conjugation length dependence of β_0 for the $[\text{Fe}_2(\eta\text{-C}_5\text{H}_5)(\text{CO})_2(\mu\text{-CO})\{\mu\text{-C-(CH=CH)}_n\text{-Fc}\}][\text{BF}_4]$ salts **13–16**

The second point of interest is that for the aromatically bridged $[\text{Fe}_2(\eta\text{-C}_5\text{H}_5)_2(\text{CO})_2(\mu\text{-CO})(\mu\text{-C-CH=CH-(ring)-CH=CH-Fc})][\text{BF}_4]$ salts the order of molecular nonlinearity decreases when the bridging aromatic ring is based on benzene (**17**) > thiophene (**18**) > furan (**19**). This result differs from those of recent studies of the second-order NLO effects in organic materials which have led to the conclusion that heterocyclic aromatic units provide

better conjugation with increased first hyperpolarisabilities than do benzenoid moieties.^[5–7] Albert et al. have demonstrated that the position of aromatic spacers within the conjugated system is important, and that in neutral molecules optimal NLO response is achieved by appending strong donors to electron-excessive spacers and strong acceptors to electron-deficient ones.^[4] Consequently it is possible that in cationic molecules the combination of the acceptor with π -deficient aromatic groups may optimise the NLO response.

However, we are not convinced that this is the whole answer, and in seeking to explain our results we note that the TLM predicts that large, frequency-independent first hyperpolarisabilities are obtained for compounds exhibiting

- a low-energy CT transition (energy E_{eg}),
- a large transition moment M which is directly correlated to the oscillator strength i.e. the extinction coefficient ϵ should be large,
- a large change in dipole moment $\Delta\mu_{\text{eg}}$, which is indicated by a pronounced solvatochromism of the CT transition.

The optical data for **17–19** show that absorption band wavelengths ($1/E_{\text{eg}}$) and intensities decrease along the series **19** > **18** > **17**, whilst the solvatochromic effect $\Delta\tilde{\nu}$ and β/β_0 increase. This is consistent with the proposal that the most important factor in determining the values of β and β_0 for these compounds is the dipole moment change during the electronic transition, $\Delta\mu_{\text{eg}}$, and that a low transition energy E_{eg} and a high transition moment M is much less important. We suggest that for these compounds increasing the ring aromaticity reduces the delocalisation of the positive charge onto the ferrocenyl group and limits it to the $\mu\text{-C-CH=CH}$ moiety in the GS but not in the ES, and thereby enhances the change in dipole moment $\Delta\mu_{\text{eg}}$ on excitation. Further support is lent to this suggestion by comparing the β_0 values of complexes **14** and **21**. The spectroscopic and X-ray data show that the CH=C(Cl) unit also reduces the delocalisation of the ferrocenyl electrons in the GS and as a consequence the β_0 value of **21** is very much larger than that of **14**. However, the same modification has a much reduced effect in the extended π -bridged complexes **20** and **22**, where the donor and acceptor are further apart and the conjugated linker includes a heterocyclic aromatic group.

Table 4. Previously reported β and β_0 values of some organometallic merocyanines for comparison with those of **13–22**

Donor	Acceptor	π -bridge	λ_{max} [nm]	$\beta \times 10^{-30}$ [esu] ^[a]	$\beta_0 \times 10^{-30}$ [esu] ^[b]	Ref.
C_6H_5	$[\text{Fe}_2(\eta\text{-C}_5\text{H}_5)(\text{CO})_2(\mu\text{-CO})(\mu\text{-C-})]^+$	$-\text{CH=CH-C}_6\text{H}_4\text{-CH=CH-}$	513	792	43	[22]
Fc	$(\eta^5\text{-C}_9\text{H}_7)\text{Ru}(\text{PPh}_3)_2$	$-\text{C}\equiv\text{C-C}\equiv\text{C-}$	345	273	141	[70]
Fc	$(\text{thiophene})\text{Mn}(\text{CO})_3^+$	$-(\text{CH=CH})_3-$	548	771 ^[c]	–34	[71]
Fc	$-\text{C(OMe)=W(CO)}_5$	$-(\text{CH=CH})_4-$		960		[76]
Fc	$-\text{C(OMe)=W(CO)}_5$	$-(\text{CH=CH})_4-$		2420 ^[d]		[76]
Fc	Azulenylm ⁺	$-\text{CH=}$	716	326	145	[77]

^[a] Measured in CH_2Cl_2 . – ^[b] Measured in THF. – ^[c] Measured in MeNO_2 . – ^[d] Measured in CH_3CN .

There have been a number of studies of NLO-active organometallic complexes utilising the ferrocene fragment as an electron donor^[71–77] and the $[\text{Fe}_2(\eta\text{-C}_5\text{H}_5)_2(\text{CO})_2(\mu\text{-CO})(\mu\text{-C-})]^+$ electron-accepting moiety.^[22,45] However, problems arise when comparing NLO values obtained from different techniques and solvents.^{[57][58]} Meaningful comparisons can only be made between our complexes and others characterised using the HRS technique at 1064 nm incident radiation (Table 4). The second-order hyperpolarisabilities presented in Table 4 confirm that the combination of ferrocenyl donor with the $[\text{Fe}_2(\eta\text{-C}_5\text{H}_5)_2(\text{CO})_2(\mu\text{-CO})(\mu\text{-C-})]^+$ acceptor is very effective as **13–22** have some of the highest β and β_0 values so far observed for organometallic compounds.

Conclusion

In summary, we have systematically modified the conjugation pathway of the cationic organometallic merocyanine system $[\text{Fe}_2(\eta\text{-C}_5\text{H}_5)_2(\text{CO})_2(\mu\text{-CO})(\mu\text{-C-CH=CH-}\{\pi\text{-linker}\}\text{-Fc})][\text{BF}_4]$ and examined the effects on the linear and nonlinear optical properties. The results agree with some previously held tenets in that extending the π -linker with olefinic units result in a bathochromic shift of the λ_{max} and concomitantly increase the second-order NLO response. However, they do not agree with others. When aromatic spacers are included, the results suggest that the first hyperpolarisabilities are optimised when the ground state delocalisation of the ferrocenyl electrons is reduced. Better results are achieved when the more aromatic benzene unit replaces thiophene or furan moieties. It appears that for our cationic merocyanines (**13–22**) a low excitation energy E_{eg} for the electronic excitation is less important than a large change in the dipole moment $\Delta\mu_{\text{eg}}$ and a large transition moment M . Furthermore, the observation that the substituent on the olefinic double bond proximate to the ferrocenyl group has a dramatic effect on the β and β_0 values (cf. **14–21**) emphasises the necessity for further rigorous and systematic research to elucidate the structure–property relationship, which is so vital for the advancement of this field.

Experimental Section

Solvent Purification and Instrumentation: Dichloromethane and THF were dried by refluxing in the presence of calcium hydride and distilled prior to use. THF was further distilled from sodium/benzophenone. Acetonitrile was dried by refluxing in the presence of calcium sulfate and distilled prior to use. – Infrared spectra were recorded with a Perkin–Elmer Paragon 1000 spectrometer. Peak positions are in cm^{-1} with relative peak heights in parentheses. – UV/Vis spectra were recorded with a Perkin–Elmer Lambda 6 spectrometer. Band positions are in nm with band intensities in parentheses. – NMR spectra were recorded with a JEOL JNM-GX 270 FT spectrometer. Chemical shifts are in ppm downfield from TMS as an internal standard and in parentheses are (multiplicity, integration, coupling constants J in Hz) where

appropriate. – Elemental analyses were carried out in the Microanalytical Laboratory, University College, Dublin.

General Procedure for the Condensation of Ferrocenyl Aldehydes 9–11 with $[\text{Fe}_2(\eta\text{-C}_5\text{H}_5)_2(\text{CO})_2(\mu\text{-CO})(\mu\text{-C-CH}_3)][\text{BF}_4]$ (12**):** Complex **12**^[37] (0.25 g, 0.57 mmol) and an excess of aldehyde (1.2 equiv.) was stirred in CH_2Cl_2 (50 mL) at 35 °C for twelve hours. The reaction mixture was filtered and the product precipitated from the filtrate by carefully adding diethyl ether (25 mL) and cooling overnight.

$[\text{Fe}_2(\eta\text{-C}_5\text{H}_5)_2(\text{CO})_2(\mu\text{-CO})(\mu\text{-C-CH=CH-Fc})][\text{BF}_4]$ (13**):** Yield 0.20 g (54%). – ^1H NMR $[(\text{CD}_3)_2\text{CO}]$: δ = 9.64 (d, 1 H, J = 14.1 Hz, $\mu\text{-C-CH}$), 8.46 (d, 1 H, J = 14.1 Hz, $\mu\text{-C-CH=CH}$), 5.55 (s, 10 H, C_5H_5), 5.42, 5.36 (C_5H_4 , Fc), 4.43 (C_5H_5 , Fc). – ^{13}C NMR $[(\text{CD}_3)_2\text{CO}]$: δ = 408.0 ($\mu\text{-C}$), 257.7 ($\mu\text{-CO}$), 209.8 (CO), 162.3, 150.9 ($\mu\text{-C-CH=CH}$), 92.1 (C_5H_5), 80.7, 80.3, 74.5, 74.0 (Fc). – IR (CH_2Cl_2): $\nu(\text{CO})$ 2024 (10.0), 1993 (2.7); $\nu(\mu\text{-CO})$ 1837 (5.4); $\nu(\text{C=C})$ 1605 (2.8), 1525 (13.2), 1461 (2.3). – UV/Vis (CH_2Cl_2): λ_{max} (ϵ) = 655 nm ($10,953 \text{ M}^{-1}\cdot\text{cm}^{-1}$), 428 nm ($17,736 \text{ M}^{-1}\cdot\text{cm}^{-1}$); (CH_3CN): λ_{max} (ϵ) = 634 ($9,390 \text{ M}^{-1}\cdot\text{cm}^{-1}$), 421 ($15,245 \text{ M}^{-1}\cdot\text{cm}^{-1}$). – $\text{C}_{26}\text{H}_{21}\text{BF}_4\text{Fe}_3\text{O}_3$ (635.8): calcd: C 49.07, H 3.30; found C 48.70, H 3.31.

$[\text{Fe}_2(\eta\text{-C}_5\text{H}_5)_2(\text{CO})_2(\mu\text{-CO})(\mu\text{-C-CH=CH-CH=CH-Fc})][\text{BF}_4]$ (14**):** Yield 0.21 g (57%). – ^1H NMR $[(\text{CD}_3)_2\text{CO}]$: δ = 9.40 (d, 1 H, J = 13.2 Hz, $\mu\text{-C-CH}$), 8.28 (d, 1 H, J = 14.1 Hz, $\mu\text{-C-CH=CH-CH=CH}$), 8.02 (t, 1 H, $\mu\text{-C-CH=CH}$), 7.06 (t, 1 H, $\mu\text{-C-CH=CH-CH}$), 5.54 (s, 10 H, C_5H_5), 5.04, 4.99 (C_5H_4 , Fc), 4.38 (C_5H_5 , Fc). – ^{13}C NMR (CD_3CN): δ = 410.5 ($\mu\text{-C}$), 257.2 ($\mu\text{-CO}$), 208.8 (CO), 163.1, 156.5, 152.6, 125.3 ($\mu\text{-C-CH=CH-CH=CH}$), 91.6 (C_5H_5), 82.1, 76.3, 72.0, 71.4 (Fc). – IR (CH_2Cl_2): $\nu(\text{CO})$ 2027 (10.0), 2001 (3.6); $\nu(\mu\text{-CO})$ 1837 (4.4); $\nu(\text{C=C})$ 1605 (2.5), 1582 (5.6), 1525 (16.7). – UV/Vis (CH_2Cl_2): λ_{max} (ϵ) = 734 ($13,881 \text{ M}^{-1}\cdot\text{cm}^{-1}$), 484 ($17,094 \text{ M}^{-1}\cdot\text{cm}^{-1}$); (CH_3CN): λ_{max} (ϵ) = 698 ($10,029 \text{ M}^{-1}\cdot\text{cm}^{-1}$), 471 ($14,397 \text{ M}^{-1}\cdot\text{cm}^{-1}$). – $\text{C}_{28}\text{H}_{23}\text{BF}_4\text{Fe}_3\text{O}_3$ (661.8): calcd: C 50.76, H 3.47; found C 46.69, H 3.82.

$[\text{Fe}_2(\eta\text{-C}_5\text{H}_5)_2(\text{CO})_2(\mu\text{-CO})(\mu\text{-C-CH=CH-CH=CH-CH=CH-Fc})][\text{BF}_4]$ (15**):** Yield 0.27 g (67%). – ^1H NMR $[(\text{CD}_3)_2\text{CO}]$: δ = 9.42 (d, 1 H, J = 13.8 Hz, $\mu\text{-C-CH}$), 7.96 (m, 2 H, $\mu\text{-C-CH=CH-CH=CH-CH=CH}$), 7.42 (d, 1 H, J = 14.6 Hz, $\mu\text{-C-CH=CH-CH=CH-CH=CH}$), 7.00 (t, 1 H, $\mu\text{-C-CH=CH-CH=CH-CH=CH}$), 6.82 (t, 1 H, $\mu\text{-C-CH=CH-CH=CH-CH=CH}$), 5.55 (s, 10 H, C_5H_5), 4.90, 4.84 (C_5H_4 , Fc), 4.33 (C_5H_5 , Fc). – ^{13}C NMR $[(\text{CD}_3)_2\text{CO}]$: δ = 413.8 ($\mu\text{-C}$), 257.1 ($\mu\text{-CO}$), 209.5 (CO), 159.2, 157.3, 154.1, 151.4, 129.8, 128.4 ($\mu\text{-C-CH=CH-CH=CH}$), 92.2 (C_5H_5), 82.3, 74.1, 71.4, 70.4 (Fc). – IR (CH_2Cl_2): $\nu(\text{CO})$ 2028 (10.0), 2000 (3.4); $\nu(\mu\text{-CO})$ 1837 (5.1); $\nu(\text{C=C})$ 1603 (3.1), 1572 (5.4), 1488 (19.5). – UV/Vis (CH_2Cl_2): λ_{max} (ϵ) = 775 ($18,277 \text{ M}^{-1}\cdot\text{cm}^{-1}$), 541 ($22,488 \text{ M}^{-1}\cdot\text{cm}^{-1}$); (CH_3CN): λ_{max} (ϵ) = 717 ($16,275 \text{ M}^{-1}\cdot\text{cm}^{-1}$), 508 ($21,034 \text{ M}^{-1}\cdot\text{cm}^{-1}$). – $\text{C}_{30}\text{H}_{25}\text{BF}_4\text{Fe}_3\text{O}_3$ (687.9): calcd: C 52.33, H 3.66; found C 52.30, H 3.92.

$[\text{Fe}_2(\eta\text{-C}_5\text{H}_5)_2(\text{CO})_2(\mu\text{-CO})(\mu\text{-C-CH=CH-CH=CH-CH=CH-Fc})][\text{BF}_4]$ (16**):** Yield 0.29 g (72%). – ^1H NMR $[(\text{CD}_3)_2\text{CO}]$: δ = 9.42 (d, 1 H, J = 13.5 Hz, $\mu\text{-C-CH}$), 7.93 (m, 2 H, $\mu\text{-C-CH=CH-CH=CH-CH=CH-CH=CH}$), 7.14 (m, 2 H, $\mu\text{-C-CH=CH-CH=CH-CH=CH-CH=CH}$), 6.77 (m, 3 H, $\mu\text{-C-CH=CH-CH=CH-CH=CH-CH=CH}$), 5.55 (s, 10 H, C_5H_5), 4.74, 4.64 (C_5H_4 , Fc), 4.25 (C_5H_5 , Fc). – ^{13}C NMR $[(\text{CD}_3)_2\text{CO}]$: δ = 415.8 ($\mu\text{-C}$), 256.9 ($\mu\text{-CO}$), 209.5 (CO), 158.9, 156.3, 154.2, 158.6, 145.2, 132.0, 131.4, 127.6 ($\mu\text{-C-CH=CH-CH=CH-CH=CH-CH=CH}$), 92.2 (C_5H_5), 82.8, 72.4,

70.8, 69.3 (Fc). – IR: (CH₂Cl₂): $\nu(\text{CO})$ 2029 (10.0), 2001 (3.5); $\nu(\mu\text{-CO})$ 1839 (5.0); $\nu(\text{C}=\text{C})$ 1606 (4.2), 1548 (6.7), 1494 (26.5). – UV/Vis: (CH₂Cl₂): λ_{max} (ϵ) = 813 (23,106 M⁻¹·cm⁻¹), 582 (24,670 M⁻¹·cm⁻¹); (CH₃CN): λ_{max} (ϵ) = 720 (14,954 M⁻¹·cm⁻¹), 521 (21,678 M⁻¹·cm⁻¹). – C₃₂H₂₇BF₄Fe₃O₃ (713.9): calcd. C 53.84, H 3.81; found C 53.54, H 3.71%.

[Fe₂(η -C₅H₅)₂(CO)₂(μ -CO)(μ -C-CH=CH-C₆H₄-CH=CH-Fc)]BF₄ (17): Yield 0.15 g (61%). – ¹H NMR (CDCl₃): δ = 9.82 (d, 1 H, J = 14.5 Hz, μ -C-CH), 8.11 (d, 2 H, J = 8.4 Hz, C₆H₄), 7.59 (hidden, μ -C-CH=CH), 7.58 (d, 2 H, J = 8.4 Hz, C₆H₄), 7.24 (hidden, C₆H₄-CH=CH), 6.71 (d, 1 H, J = 16.0 Hz, C₆H₄-CH=CH), 5.29 (s, 10 H, C₅H₅), 4.60, 4.48 (C₅H₄, Fc), 4.21 (C₅H₅, Fc). – ¹³C NMR (CDCl₃): δ = 431.6 (μ -C), 255.1 (μ -CO), 207.7 (CO), 153.1, 151.7 (μ -C-CH=CH), 134.4, 127.8, 133.4, 125.8 (C₆H₄-CH=CH), 132.8, 131.0 (C q -C₆H₄), 92.1 (C₅H₅), 71.3, 72.1, 70.9 (Fc). – IR: (CH₂Cl₂): $\nu(\text{CO})$ 2035 (10.0), 2004 (2.7); $\nu(\mu\text{-CO})$ 1844 (5.2); $\nu(\text{C}=\text{C})$ 1605 (4.4), 1593 (4.6), 1556 (4.6), 1527 (11.5), 1506 (7.7), 1456 (2.8). – UV/Vis (CH₂Cl₂): λ_{max} (ϵ) = 705 (12,162 M⁻¹·cm⁻¹), 512 (28,692 M⁻¹·cm⁻¹); (CH₃CN): λ_{max} (ϵ) = 616 (12,803 M⁻¹·cm⁻¹), 480 (26,773 M⁻¹·cm⁻¹). – C₃₄H₂₇BF₄Fe₃O₃ (737.9): calcd. C 55.28, H 3.66; found C 53.87, H 3.85.

[Fe₂(η -C₅H₅)₂(CO)₂(μ -CO)(μ -C-CH=CH-C₄H₂S-CH=CH-Fc)]BF₄ (18): Yield 0.22 g (52%). – ¹H NMR (CD₃CN): δ = 9.24 (d, 1 H, J = 13.8 Hz, μ -C-CH), 8.49 (d, 1 H, J = 3.9 Hz, C₂H₄S), 7.95 (d, 1 H, J = 13.8 Hz, μ -C-CH=CH), 7.24 (d, 1 H, J = 15.2 Hz, C₂H₄S-CH=CH-Fc), 7.12 (d, 1 H, J = 3.9 Hz, C₂H₄S), 6.82 (d, 1 H, J = 15.2 Hz, C₂H₄S-CH=CH-Fc), 5.21 (s, 10 H, C₅H₅), 4.72, 4.64 (C₅H₄, Fc), 4.31 (C₅H₅, Fc). – ¹³C NMR (CDCl₃): δ = 409.5 (μ -C), 256.9 (μ -CO), 209.4 (CO), 160.4, 138.3 (C q -C₂H₄S), 149.7, 146.6, 146.3, 138.4, 123.0, 119.2 (μ -C-CH=CH; C³, C⁴-C₂H₄S; C₂H₄S-CH=CH-Fc), 92.8 (C₅H₅), 82.2, 76.2, 70.5, 69.2 (Fc). – IR: CH₂Cl₂: $\nu(\text{CO})$ 2030 (10.0), 1999 (3.4); $\nu(\mu\text{-CO})$ 1839 (5.3); $\nu(\text{C}=\text{C})$ 1604 (5.9), 1529 (14.9), 1493 (4.9). – UV/Vis (CH₂Cl₂): λ_{max} (ϵ) = 757 (19,966 M⁻¹·cm⁻¹), 569 (32,538 M⁻¹·cm⁻¹); (CH₃CN): λ_{max} (ϵ) = 688 (17,147 M⁻¹·cm⁻¹), 542 (26,378 M⁻¹·cm⁻¹). – C₃₂H₂₅BF₄Fe₃O₃S (744.0): calcd. C 51.61, H 3.36; found C 54.85, H 3.95.

[Fe₂(η -C₅H₅)₂(CO)₂(μ -CO)(μ -C-CH=CH-C₄H₂O-CH=CH-Fc)]BF₄ (19): Yield 0.23 g (55.6%). – ¹H NMR (CD₃CN): δ = 9.64 (d, 1 H, J = 13.9 Hz, μ -C-CH), 7.92 (br. s, C₂H₄O), 7.82 (d, 1 H, J = 15.8 Hz, C₂H₄O-CH=CH-Fc), 7.61 (d, 1 H, J = 13.9 Hz, μ -C-CH=CH), 6.95 (d, 1 H, J = 3.9 Hz, C₂H₄O), 6.87 (d, 1 H, J = 15.8 Hz, C₂H₄O-CH=CH-Fc), 5.39 (s, 10 H, C₅H₅), 4.79, 4.68 (C₅H₄, Fc), 4.31 (C₅H₅, Fc). – ¹³C NMR (CD₃CN): δ = 406.8 (μ -C), 258.1 (μ -CO), 209.8 (CO), 165.9, 147.5 (C q -C₂H₄O), 147.4, 141.3, 137.5, 136.1, 117.1, 113.3 (μ -C-CH=CH; C³, C⁴-C₂H₄O; C₂H₄O-CH=CH-Fc), 92.3 (C₅H₅), 82.6, 7.35, 7.45, 70.0 (Fc). – IR: CH₂Cl₂: $\nu(\text{CO})$ 2029 (10.0), 2000 (3.3); $\nu(\mu\text{-CO})$ 1838 (5.1); $\nu(\text{C}=\text{C})$ 1605 (7.5), 1560 (1.7), 1529 (12.7), 1493 (5.1). – UV/Vis: (CH₂Cl₂): λ_{max} (ϵ) = 747 (22,325 M⁻¹·cm⁻¹), 577 (33,211 M⁻¹·cm⁻¹); (CH₃CN): λ_{max} (ϵ) = 683 (21,202 M⁻¹·cm⁻¹), 551 (28,946 M⁻¹·cm⁻¹). – C₃₂H₂₅BF₄Fe₃O₄ (727.9): calcd. C 52.75, H 4.43; found C 51.48, H 3.72.

[Fe₂(η -C₅H₅)₂(CO)₂(μ -CO)(μ -C-CH=CH-C₄H₂S-CH=CH-CH=CH-Fc)]BF₄ (20): Yield 0.21 g (49%). – ¹H NMR [(CD₃)₂CO]: δ = 9.75 (d, 1 H, J = 14.1 Hz, μ -C-CH), 8.33 (d, 1 H, J = 14.1 Hz, μ -C-CH=CH), 8.27 (d, 1 H, J = 4.2 Hz, C₂H₄S), 7.49 (d, 1 H, J = 4.2 Hz, C₂H₄S), 7.27 (dd, 1 H, J = 15.2, 10.69 Hz, C₂H₄S-CH=CH-CH=CH-Fc), 6.94 (d, 1 H, J = 15.2 Hz, C₂H₄S-CH=CH-CH=CH-Fc), 6.91 (d, 1 H, J = 15.5 Hz, C₂H₄S-CH=CH-CH=CH-Fc), 6.77 (dd, 1 H, J = 15.5,

10.7 Hz, C₂H₄S-CH=CH-CH=CH-Fc), 5.60 (C₅H₅), 4.67, 4.52 (C₅H₄, Fc), 4.22 (C₅H₅, Fc). – ¹³C NMR [(CD₃)₂CO]: δ = 414.1 (μ -C), 255.6 (μ -CO), 208.3 (CO), 159.0, 137.8 (C q -C₂H₄S), 148.7, 145.2, 144.5, 139.1, 136.9, 129.4, 126.0, 121.8 (μ -C-CH=CH; C³, C⁴-C₂H₄S; C₂H₄S-CH=CH-CH=CH-Fc), 91.2 (C₅H₅), 83.4, 70.6, 69.7, 67.7 (Fc). – IR: CH₂Cl₂: $\nu(\text{CO})$ 2030 (10.0), 2000 (2.5); $\nu(\mu\text{-CO})$ 1839 (5.1); $\nu(\text{C}=\text{C})$ 1604 (6.1), 1586 (3.0), 1528, (16.8), 1490 (4.0). – UV/Vis: (CH₂Cl₂): λ_{max} (ϵ) = 764 (22,363 M⁻¹·cm⁻¹), 606 (29,169 M⁻¹·cm⁻¹); (CH₃CN): λ_{max} (ϵ) = 677 (19,199 M⁻¹·cm⁻¹), 590 (30,565 M⁻¹·cm⁻¹). – C₃₄H₂₇BF₄Fe₃O₃S (770.0): calcd. C 52.99, H 3.51; found C 48.93, H 3.69.

[Fe₂(η -C₅H₅)₂(CO)₂(μ -CO)(μ -C-CH=CH-CH=C(Cl)-Fc)]BF₄ (21): Yield 0.25 g (61.9%). – ¹H NMR [(CD₃)₂CO]: δ = 9.29 (d, 1 H, J = 13.8 Hz, μ -C-CH), 7.85 (dd, 1 H, J = 11.5, 13.8 Hz, μ -C-CH=CH), 7.14 (d, 1 H, J = 11.5 Hz, μ -C-CH=CH-CH), 5.33 (s, 10 H, C₅H₅), 5.12, 5.00 (C₅H₄, Fc), 4.35 (C₅H₅, Fc). – ¹³C NMR (CD₃CN): δ = 422.5 (μ -C), 255.6 (μ -CO), 208.6 (CO), 160.7 [μ -C-CH=CH-CH=C(Cl)], 153.2, 148.1, 121.7 (μ -C-CH=CH-CH), 92.0 (C₅H₅), 83.0, 76.0, 72.7, 70.9 (Fc). – IR: CH₂Cl₂: $\nu(\text{CO})$ 2031 (10.0), 2001 (2.3); $\nu(\mu\text{-CO})$ 1841 (4.4); $\nu(\text{C}=\text{C})$ 1605 (1.4), 1553 (4.6), 1521 (13.1). – UV/Vis: (CH₂Cl₂): λ_{max} (ϵ) = 746 (17,173 M⁻¹·cm⁻¹), 495 (27,589 M⁻¹·cm⁻¹); (CH₃CN): λ_{max} (ϵ) = 713 (13,986 M⁻¹·cm⁻¹), 477 (24,439 M⁻¹·cm⁻¹). – C₂₈H₂₂BClF₄Fe₃O₃ (696.3): calcd. C 48.24, H 3.16; found C 47.74, H 3.43.

[Fe₂(η -C₅H₅)₂(CO)₂(μ -CO)(μ -C-CH=CH-C₄H₂S-CH=CH-CH=C(Cl)-Fc)]BF₄ (22): Yield 0.26 g (56.9%). – ¹H NMR [(CD₃)₂CO]: δ = 9.85 (1 H, d, J = 14.4 Hz, μ -C-CH), 8.34 (d, 1 H, J = 14.3 Hz, μ -C-CH=CH), 8.26 (d, 1 H, J = 3.7 Hz, C₂H₄S), 7.54 (d, 1 H, J = 3.7 Hz, C₂H₄S), 7.44 [dd, 1 H, J = 15.2, 10.7 Hz, C₂H₄S-CH=CH-CH=C(Cl)-Fc], 7.17 [d, 1 H, J = 15.2 Hz, C₂H₄S-CH=CH-CH=C(Cl)-Fc], 7.02 [d, 1 H, J = 10.7 Hz, C₂H₄S-CH=CH-CH=C(Cl)-Fc], 5.64 (C₅H₅), 4.82, 4.54 (C₅H₄, Fc), 4.26 (C₅H₅, Fc). – ¹³C NMR ((CD₃)₂CO): δ = 420.8 (μ -C), 256.2 (μ -CO), 209.4 (CO), 158.2, 139.8, 139.4 [C q -C₂H₄S; C₂H₄S-CH=CH-CH=C(Cl)-Fc], 150.3, 145.8, 145.2, 131.6, 131.4, 125.9, 122.1 [μ -C-CH=CH; C³, C⁴-C₂H₄S; C₂H₄S-CH=CH-CH=C(Cl)-Fc], 92.6 (C₅H₅), 84.3, 71.8, 71.2, 68.7 (Fc). – IR: CH₂Cl₂: $\nu(\text{CO})$ 2031 (10.0), 2001 (2.3); $\nu(\mu\text{-CO})$ 1840 (5.0); $\nu(\text{C}=\text{C})$ 1605 (1.7), 1583 (2.7), 1528 (16.6), 1490 (4.3). – UV/Vis: (CH₂Cl₂): λ_{max} (ϵ) = 731 (24,000 M⁻¹·cm⁻¹), 606 (34,798 M⁻¹·cm⁻¹); (CH₃CN): λ_{max} (ϵ) = 644 (30,695 M⁻¹·cm⁻¹), 572 (36,213 M⁻¹·cm⁻¹). – C₃₄H₂₆BClF₄Fe₃O₃S (804.4): calcd. C 50.71, H 3.23; found C 49.44, H 3.50.

X-ray Structure Determination of 21: Crystals suitable for an X-ray structure analysis were obtained by diffusion of Et₂O into a CH₂Cl₂ solution of **21**. The data were collected with a four-circle Hilger & Watts diffractometer, Mo-K α , λ = 0.71073 Å. The structure was resolved by direct methods (SHELXL-86).^[78] Refinement on F^2 was carried out by full-matrix least-squares techniques (SHELXL-93).^[79] All non-hydrogen atoms were refined with anisotropic thermal parameters. The hydrogen atoms were refined with a fixed isotropic thermal parameter related by a factor of 1.2 to the value of the equivalent isotropic thermal parameter of their carrier atoms. Weights were optimised in the final refinement cycles. Crystal data and structure refinement are given Table 5, whilst selected bond lengths [pm] and angles [°] are listed in Table 1. Crystallographic data (excluding structure factors) for the reported structure have been deposited with the Cambridge Crystallographic Data Centre as supplementary publication no. CCDC-149412. Copies of the data can be obtained free of charge on application

to CCDC, 12 Union Road, Cambridge CB2 1EZ, UK [Fax: (internat.) + 44 1223/336-033; E-mail: deposit@ccdc.cam.ac.uk].

Table 5. Crystal data and structure refinement for $[\text{Fe}_2(\eta\text{-C}_5\text{H}_5)_2(\text{CO})_2(\mu\text{-CO})\{\mu\text{-C}-\text{CH}=\text{CH}-\text{CH}=\text{C}(\text{Cl})-\text{Fc}\}][\text{BF}_4]$ (**21**)

Empirical formula	$\text{C}_{28}\text{H}_{22}\text{BClF}_4\text{Fe}_3\text{O}_3$
Molecular mass [g/mol]	696.27
Temperature [K]	173
λ [pm]	7.1073
Crystal system	monoclinic
Space group	$P2_1/c$
Unit cell dimensions [\AA , $^\circ$]	$a = 8.846(4)$ $b = 24.087(8)$ $c = 13.025(4)$ $\beta = 97.90(3)$
V [\AA^3]	2749.0(17)
Z	4
$\rho_{\text{calcd.}}$ [g/cm^3]	1.682
Absorption coefficient [mm^{-1}]	1.716
$F(000)$	1400
Crystal size [mm]	$0.6 \times 0.4 \times 0.3$
$\theta_{\text{min}}-\theta_{\text{max}}$ [$^\circ$]	$2.31-25.07$
Index ranges	$-1 \leq h \leq 10$ $0 \leq k \leq 28$ $-15 \leq l \leq 15$
Collected reflections	5382
Unique reflections	4882
R_{int}	0.0245
Data [$I > 4\sigma(I)$]	4882
Parameters	361
Goodness-of-fit	1.045
$R1/wR2$ [$I > 2\sigma(I)$]	0.0390/0.0986
$R1/wR2$ (all data)	0.0489/0.1040
min./max. residual electron density [$\text{e}\cdot\text{\AA}^{-3}$]	$-0.552, 0.612$

HRS Measurements of the First Hyperpolarisabilities: Experimental setup details can be found in ref.^[56] An Nd:YAG laser with a wavelength of 1064 nm was used as incident light source. All measurements were carried out in dry CH_2Cl_2 with sample concentrations of 10^{-6} to 10^{-4} M using *p*-NA as the external reference [$\beta(\text{CH}_2\text{Cl}_2) = 21.6 \cdot 10^{-30}$ esu^[56]]. The compounds were checked for fluorescence using the bandpass filter method described in ref.^[22]

Acknowledgments

This work was supported by the European Community through the TMR Network Contract No. ERBFMRX-CT98-0166.

- [1] D. R. Kanis, M. A. Ratner, T. J. Marks, *Chem. Revs.* **1994**, *94*, 195.
 [2] L.-T. Cheng, W. Tam, S. H. Stevenson, G. R. Meredith, G. Rikken, S. R. Marder, *J. Phys. Chem.* **1991**, *95*, 10631.
 [3] L.-T. Cheng, W. Tam, S. R. Marder, A. E. Stiegman, G. Rikken, C. W. Spangler, *J. Phys. Chem.* **1991**, *95*, 10643.
 [4] I. D. L. Albert, T. J. Marks, M. A. Ratner, *J. Am. Chem. Soc.* **1997**, *119*, 6575.
 [5] A. K.-Y. Jen, V. Pushkara Rao, K. Y. Wong, K. J. Drost, *J. Chem. Soc., Chem. Commun.* **1993**, 90.
 [6] V. Pushkara Rao, A. K.-Y. Jen, K. Y. Wong, K. J. Drost, *J. Chem. Soc., Chem. Commun.* **1993**, 1118.
 [7] A. K.-Y. Jen, Y. Cai, P. V. Bedworth, S. R. Marder, *Adv. Mater.* **1997**, *9*, 132.
 [8] S. R. Marder, J. W. Perry, B. G. Tiemann, *Organometallics* **1991**, *10*, 1896.

- [9] V. Alain, M. Blanchard-Desce, C.-T. Chen, S. R. Marder, A. Fort, M. Barzoukas, *Synth. Met.* **1996**, *81*, 133.
 [10] C. Lambert, W. Gaschler, M. Zabel, R. Matschiner, R. Wortmann, *J. Organomet. Chem.* **1999**, *592*, 109.
 [11] T. J. J. Müller, A. Netz, M. Ansorge, *Organometallics* **1999**, *18*, 5066.
 [12] H. Wong, T. Meyer-Friedrichsen, T. Farrell, C. Mecker, J. Heck, *Eur. J. Inorg. Chem.* **2000**, 631 and reference [1] therein.
 [13] I. R. Whittall, A. M. McDonagh, M. G. Humphrey, *Adv. Organomet. Chem.* **1998**, *42*, 291.
 [14] T. Saji, I. Kinoshita, *J. Chem. Soc., Chem. Commun.* **1986**, 716.
 [15] J. Malthete, J. Billard, *Mol. Cryst. Liq. Cryst.* **1976**, *34*, 117.
 [16] R. Deschenaux, J. Santiago, *J. Mater. Chem.* **1993**, *3*, 219.
 [17] M. B. Hall, R. F. Fenske, *Inorg. Chem.* **1972**, *11*, 768.
 [18] C. P. Casey, M. S. Konings, S. R. Marder, Y. Takezawa, *J. Organomet. Chem.* **1988**, *358*, 347.
 [19] C. P. Casey, M. S. Konings, S. R. Marder, *Polyhedron* **1988**, *7*, 881.
 [20] C. P. Casey, M. S. Konings, S. R. Marder, *J. Organomet. Chem.* **1988**, *345*, 125.
 [21] J. A. Bandy, H. E. Bunting, M.-H. Garcia, M. L. H. Green, S. R. Marder, M. E. Thompson, *Polyhedron* **1992**, *12*, 1429.
 [22] T. Farrell, T. Meyer-Friedrichsen, J. Heck, A. R. Manning, *Organometallics* **2000**, *19*, 3410.
 [23] S. R. Marder, J. W. Perry, *Adv. Mater.* **1993**, *5*, 804.
 [24] C.-T. Chen, S. R. Marder, L.-T. Cheng, *J. Chem. Soc., Chem. Commun.* **1994**, 259.
 [25] S. R. Marder, D. N. Beratan, L.-T. Cheng, *Science* **1991**, *252*, 103.
 [26] S. R. Marder, B. Kippelen, A. K. Jen, N. Peyghambarian, *Nature* **1997**, *388*, 845.
 [27] D. Lednicer, C. R. Hauser, *Org. Synth.* **40**, 31.
 [28] P. L. Pauson, W. E. Watts, *J. Chem. Soc.* **1963**, 1990.
 [29] T. Farrell, Ph.D. Thesis, University College Dublin, **1998**.
 [30] J. M. Barker, P. R. Huddleston, M. L. Wood, *Synth. Commun.* **1975**, *5*, 65.
 [31] R. Guillard, P. Fournai, M. Person, *Bull. Soc. Chim. Fr.* **1967**, *11*, 4121.
 [32] R. Antonioletti, M. D'Auria, G. Piancatelli, A. Scettri, *J. Chem. Soc., Perkin Trans. 1* **1985**, 1285.
 [33] D. J. Chadwick, J. Chambers, G. D. Meakins, R. L. Snowden, *J. Chem. Soc., Perkin Trans. 1* **1973**, 1766.
 [34] G. D. Broadhead, J. M. Osgerby, P. L. Pauson, *J. Chem. Soc.* **1958**, 650.
 [35] M. Rosenblum, N. Braun, J. Papenmeier, M. Applebaum, *J. Organomet. Chem.* **1966**, *15*, 173.
 [36] C. W. Spangler, R. K. McCoy, *Synth. Commun.* **1988**, *18*, 51.
 [37] M. Nitay, W. Priester, M. Rosenblum, *J. Am. Chem. Soc.* **1978**, *100*, 3620.
 [38] C. P. Casey, M. S. Konings, R. E. Palermo, R. E. Colborn, *J. Am. Chem. Soc.* **1985**, *107*, 5296.
 [39] M. Etienne, J. Talarmin, L. Toupet, *Organometallics* **1992**, *11*, 2058.
 [40] G. Bourhill, J. L. Bredas, L. T. Cheng, S. R. Marder, F. Meyers, J. W. Perry, B. G. Tiemann, *J. Am. Chem. Soc.* **1994**, *116*, 2619.
 [41] S. R. Marder, L. T. Cheng, B. G. Tiemann, A. C. Friedli, M. Blanchard-Desce, J. W. Perry, J. Skindhoj, *Science* **1994**, *263*, 511.
 [42] C. P. Casey, M. S. Konings, S. R. Marder, *Polyhedron* **1988**, *7*, 881.
 [43] C. P. Casey, M. S. Konings, S. R. Marder, *J. Organomet. Chem.* **1988**, *345*, 125.
 [44] C. P. Casey, M. S. Konings, S. R. Marder, Y. Takezawa, *J. Organomet. Chem.* **1988**, *358*, 347.
 [45] J. A. Bandy, H. E. Bunting, M.-H. Garcia, M. L. H. Green, S. R. Marder, M. E. Thompson, *Polyhedron* **1992**, *12*, 1429.
 [46] J. A. Campo, M. Cano, J. V. Heras, C. Lopez-Garabito, E. Pinilla, R. Torres, G. Rojo, F. Agullo-lopez, *J. Mater. Chem.* **1999**, *9*, 899.

- [47] B. J. Coe, C. J. Jones, J. A. McCleverty, D. Bloor, G. Cross, *J. Organomet. Chem.* **1994**, 464, 225.
- [48] A. Houlton, J. Naseralla, R. M. G. Roberts, J. Silver, D. Cunningham, P. McArdle, T. Higgins, *J. Chem. Soc., Dalton Trans.* **1992**, 2236.
- [49] S. R. Marder, J. W. Perry, B. G. Tiemann, W. P. Schaefer, *Organometallics* **1991**, 10, 1896.
- [50] C. Reichardt, *Solvents and Solvent Effects in Organic Chemistry*, 2nd ed., VCH, Weinheim, **1988**.
- [51] J. C. Calabrese, L.-T. Cheng, J. C. Green, S. R. Marder, W. Tam, *J. Am. Chem. Soc.* **1991**, 113, 7227.
- [52] D. R. Kanis, M. A. Ratner, T. J. Marks, *J. Am. Chem. Soc.* **1992**, 114, 10338.
- [53] S. Barlow, B. E. Bunting, C. Ringham, J. C. Green, G. U. Bublitz, S. G. Boxer, I. W. Perry, S. R. Marder, *J. Am. Chem. Soc.* **1999**, 121, 3715.
- [54] J. L. Oudar, D. S. Chemla, *Chem. Phys.* **1977**, 66, 2664.
- [55] E. Hendrickx, K. Clays, A. Persoons, C. Dehu, J. L. Bredas, *J. Am. Chem. Soc.* **1995**, 363, 58.
- [56] K. Clays, A. Persoons, *Rev. Sci. Instrum.* **1992**, 63, 3285.
- [57] J. J. Wolff, R. Wortmann, *Adv. Phys. Org. Chem.* **1999**, 121.
- [58] K. Clays, E. Hendrickx, T. Verbiest, A. Persoons, *Adv. Mater.* **1998**, 10, 643.
- [59] J. J. Wolff, R. Wortmann, *J. Prakt. Chem.* **1998**, 340, 99.
- [60] S. Stadler, G. Bourhill, C. Bräuchle, *J. Phys. Chem.* **1996**, 100, 6927.
- [61] M. C. Flipse, R. De Jonge, R. H. Woudenberg, A. W. Marsman, C. A. Van Walree, L. W. Jenneskens, *Chem. Phys. Letts.* **1995**, 245, 297.
- [62] S. K. Pal, A. Krishnan, K. D. Puspendu, A. G. Samuelson, *J. Organomet. Chem.* **2000**, 604, 248.
- [63] S. Stadler, R. Dietrich, G. Bourhill, C. Bräuchle, A. Pawlik, W. Grahn, *Chem. Phys. Lett.* **1995**, 247, 271.
- [64] M. A. Pauley, C. H. Wang, *Rev. Sci. Instrum.* **1999**, 70, 3285.
- [65] S. Stadler, R. Dietrich, G. Bourhill, C. Bräuchle, *Opt. Lett.* **1996**, 21, 251.
- [66] O. F. J. Noordman, N. F. van Hulst, *Chem. Phys. Lett.* **1996**, 253, 145.
- [67] G. Olbrechts, R. Strobbe, K. Clays, A. Persoons, *Rev. Sci. Instrum.* **1998**, 69, 2233.
- [68] N. W. Song, T.-I. Kang, S. C. Jeoung, S.-J. Jeon, B. R. Cho, D. Kim, *Chem. Phys. Lett.* **1996**, 261, 307.
- [69] O. K. Song, J. N. Woodford, C. H. Wang, *J. Phys. Chem. A* **1997**, 101, 3222.
- [70] V. Cadiero, S. Conejero, M. P. Camasa, J. Gimeno, I. Asselberghs, S. Houbrechts, K. Clays, A. Persoons, J. Borge, S. Garcia-Granda, *Organometallics* **1999**, 18, 582.
- [71] I. S. Lee, H. Seo, Y. K. Chung, *Organometallics* **1999**, 18, 1091.
- [72] O. Briel, K. Sünkel, I. Krossing, H. Nöth, E. Schmälzlin, K. Meerholz, C. Bräuchle, W. Beck, *Eur. J. Inorg. Chem.* **1999**, 483.
- [73] I. S. Lee, S. S. Lee, H. Seo, Y. K. Chung, *Inorg. Chim. Acta.* **1998**, 279, 243.
- [74] J. Mata, S. Uriel, E. Peris, R. Llusar, S. Houbrechts, A. Persoons, *J. Organomet. Chem.* **1998**, 562, 197.
- [75] E. Hendrickx, A. Persoons, S. Samson, G. R. Stephenson, *J. Organomet. Chem.* **1997**, 542, 295.
- [76] K. N. Jayaprakash, P. C. Ray, I. Matsuoka, M. M. Bhadhbade, V. G. Puranik, P. K. Das, H. Nishihara, A. Sarkar, *Organometallics* **1999**, 18, 3851.
- [77] T. Farrell, T. Meyer-Friedrichsen, M. Malessa, D. Haase, W. Saak, I. Asselberghs, K. Wostyn, K. Clays, A. Persoons, J. Heck, A. R. Manning, *J. Chem. Soc., Dalton Trans.*, in press.
- [78] G. M. Sheldrick, *SHELXS-86 Program for crystal structure determination*. University of Göttingen, Germany, **1986**.
- [79] G. M. Sheldrick, *SHELXL-93 Program for crystal structure refinement*. University of Göttingen, Germany, **1993**.

Received September 12, 2000

[I00341]